Proc. Natl. Acad. Sci. USA
Vol. 86, pp. 9642–9646, December 1989
Biochemistry

Evolution of a bifunctional enzyme: 6-Phosphofructo-2-kinase/fructose-2,6-bisphosphatase

(phosphoglycerate mutase/acid phosphatase/nucleotide-binding fold/protein-structure prediction/molecular modeling)

J. FERNANDO BAZAN*, ROBERT J. FLETTERICK*, AND SIMON J. PILKIS†

*Department of Biochemistry and Biophysics, University of California, San Francisco, CA 94143; and †Department of Physiology and Biophysics, State University of New York, Stony Brook, NY 11794

Communicated by Ora M. Rosen, July 27, 1989 (received for review June 24, 1989)

ABSTRACT **The bifunctional rat liver enzyme 6-phosphofructo-2-kinase/fructose-2,6-bisphosphatase (ATP:D-fructose-6-phosphate 2-phosphotransferase/D-fructose-2,6-bisphosphate 2-phosphohydrolase, EC 2.7.1.105/EC 3.1.3.46) is constructed of two independent catalytic domains. We present evidence that the kinase and bisphosphatase halves of the bifunctional enzyme are, respectively, structurally similar to the glycolytic enzymes 6-phosphofructo-1-kinase and phosphoglycerate mutase. Computer-assisted modeling of the C-terminal bisphosphatase domain reveals a hydrophobic core and active site residue constellation equivalent to the yeast mutase structure; structural differences map to length-variable, surface-located loops. Sequence patterns derived from the structural alignment of mutases and the bisphosphatase further detect a significant similarity to a family of acid phosphatases. The N-terminal kinase domain, in turn, is predicted to form a nucleotide-binding fold that is analogous to a segment of 6-phosphofructo-1-kinase, suggesting that these unrelated enzymes bind fructose 6-phosphate and ATP substrates in a similar geometry. This analysis indicates that the bifunctional enzyme is the likely product of gene fusion of kinase and mutase/phosphatase catalytic units.**

The bifunctional enzyme 6-phosphofructo-2-kinase/fructose-2,6-bisphosphatase (6-*P*F-2K/Fru-2,6-P_2ase; ATP:D-fructose-6-phosphate 2-phosphotransferase/D-fructose-2,6 bisphosphate 2-phosphohydrolase, EC 2.7.1.105/3.1.3.46) catalyzes both the synthesis and degradation of fructose 2,6-bisphosphate (Fru-2,6-P_2), a potent regulator of 6-phosphofructo-1-kinase (6-*P*F-1-K) and fructose-1,6-bisphosphatase (1, 2). The two opposing reactions catalyzed by 6-*P*F-2-K/Fru-2,6-P_2ase are believed to occur at two discrete active sites (3). In support of this view, protein modification experiments with selective chemical reagents or proteases have differential effects on the two reactions (4). Furthermore, cAMP-dependent protein-kinase-catalyzed phosphorylation of the enzyme results in inhibition of the kinase and activation of the bisphosphatase (P_2ase) (5, 6).

The 470-amino acid sequence of mature 6-*P*F-2-K/Fru-2,6-P_2ase from rat liver revealed a fragmentary similarity of the chain encircling His-258 (7) with that surrounding the active-site His-8 of yeast phosphoglycerate mutase (PGM) (8). His-8 in yeast PGM is transiently phosphorylated during catalysis (9). The analogous His-258 residue in rat 6-*P*F-2-K/Fru-2,6-P_2ase is likewise phosphorylated during the hydrolysis of Fru-2,6-P_2 in the P_2ase reaction (10), suggesting that the observed sequence similarity has a strong functional correlation. In this work, we show that the C-terminal P_2ase domain of the rat enzyme (Fru-2,6-P_2ase), residues 250–470, can be modeled on the known three-dimensional structure of the distantly related yeast PGM (11). This homology is proposed to extend to acid phosphatases (*P*ases), enzymes that catalyze similar phosphotransfer reactions and also use a phosphohistidine intermediate (12).

Structural analysis of the N-terminal region of the rat enzyme (residues 1–249) shows that a segment is consistent with a nucleotide-binding fold (nbf) (13), suggesting that it forms the kinase domain (6-*P*F-2-K). We argue that the likely folding topology of rat 6-*P*F-2-K is analogous to a domain of 6-*P*F-1-K (14). However, significant departures of the kinase model from the 6-*P*F-1-K structure argue for the independent evolution of 6-*P*F-2-K.

METHODS

Many of the techniques and tools used in this analysis have been described for another exercise (15). A more detailed structural study of 6-*P*F-2-K/Fru-2,6-P_2ase will be presented elsewhere (16). The University of Wisconsin Genetics Computer Group (ref. 17, release 5.2) package of biosequence analysis programs was used to assemble the alignments in Figs. 1–4. The PROFILE program of Gribskov *et al.* (18) was particularly useful in deriving structurally based sequence patterns characteristic of the P_2ase/mutase fold. Taylor (19) reviews the success of linking pattern-matching and structure-prediction algorithms in sequence comparisons.

Protein tertiary structure modeling of the P_2ase and kinase domains of 6-*P*F-2-K/Fru-2,6-P_2ase was carried out on an Evans & Sutherland PS390 graphics workstation with the INSIGHT (Biosym Technologies, San Diego, CA) and FRODO (20) software packages. X-ray coordinates for yeast PGM (11), *Bacillus Stearothermophilus* 6-*P*F-1-K (14), and *Escherichia coli* 6-*P*F-1-K bound to products (21) are available from the Protein Data Bank (22). The yeast PGM fold served as a template for the Fru-2,6-P_2ase structure. Replacement of P_2ase residues onto the mutase core (163 spatially equivalent amino acids) proceeded systematically with distinction of identical, conservative, semiconservative, and nonconservative changes (16). INSIGHT maximizes the spatial overlap of new and old amino acids; rotamer libraries determine placement of unmatched atoms (23). Reassuringly, spatially equivalent amino acids in homologous proteins tend to have significant side-chain overlaps (24). The major structural adjustments were loop deletions to the original yeast PGM structure: residues 22–23, 69–75, 170–172, and 206. Crafting of the new P_2ase loops was done by hand; FRODO (20) regularization routines then served to relieve the steric and torsional stresses brought about by side-chain replacements and reannealing of shortened surface loops.

The publication costs of this article were defrayed in part by page charge payment. This article must therefore be hereby marked "*advertisement*" in accordance with 18 U.S.C. §1734 solely to indicate this fact.

Abbreviations: Fru-6-*P*, fructose 6-phosphate; Fru-1,6-P_2, fructose 1,6-bisphosphate; Fru-2,6-P_2, fructose 2,6-bisphosphate; Fru-2,6-P_2ase, fructose-2,6-bisphosphatase; 6-*P*F-2-K, 6-phosphofructo-2-kinase; 6-*P*F-2-K/Fru-2,6-P_2ase, 6-phosphofructo-2-kinase/fructose-2,6-bisphosphatase; 6-*P*F-1-K, 6-phosphofructo-1-kinase; PGM, phosphoglycerate mutase; BPGM, bisphosphoglycerate mutase; acid Pase, acid phosphatase; nbf, nucleotide-binding fold.

RESULTS

The P_2ase Domain Is Homologous to Mutases. The yeast PGM structure is a typical three-layer α/β fold: a largely parallel β-sheet core sandwiched by α-helices (11). The active site of the mutase lies in a crevice at the C-terminal end of the β-sheet (11), a site topologically favored in nbf-like structures for binding nucleotides and other negatively charged ligands (25). PGM does not bind nucleotides but favors the nbf-like α/β structure for binding phosphoglycerates and for the spatial grouping of catalytic residues far apart in sequence. In particular, His-179 is juxtaposed with the phosphorylated His-8 in the yeast PGM tertiary structure (11). This ≈170-amino acid spacing between active site histidines is closely reproduced in the related human muscle and brain PGM isozymes (26–28) and the human, rabbit, and mouse bisphosphoglycerate mutase enzymes (BPGM) (29–31).

We propose that the mutase-analogous catalytic histidine chain spacing in the rat Fru-2,6-P_2ase domain is 134 residues; His-392 is the likely companion to His-258 in the P_2ase active site (Fig. 1). This assignment is the result of a secondary structural study that located similar α and β secondary elements in Fru-2,6-P_2ase to those found in yeast PGM (11) or were predicted to occur in the other homologous mutases. The complete structural alignment of these seven proteins requires introducing several gaps in the shorter Fru-2,6-P_2ase sequence that map to exposed surface loops in the yeast PGM structure (Fig. 1). The largest gap localizes to a long meandering loop in the mutase structure between core strand *C* and helix **4**. Residues 333–361 of Fru-2,6-P_2ase map to a 25-amino-acid-longer chain of yeast PGM (residues 92–145) that represents a large excursion from the core α/β mutase fold (Fig. 2*A*) (11). This region of the yeast PGM structure forms a loosely packed lobe that overhangs the active-site crevice (11). The analogous but shorter excursion in Fru-2,6-P_2ase probably adopts a different conformation than in yeast PGM and is therefore not in structural alignment with the mutases in Fig. 1 (see Fig. 2*B*).

A crucial structural idiosyncrasy in helix **4** of the yeast PGM structure (which precedes His-179) is conserved in rat Fru-2,6-P_2ase: helix **4** is "kinked" by Pro-160, allowing close packing of the long helix to the curled β-sheet core (11). The analogous helix **4** in Fru-2,6-P_2ase is bent by Pro-376 (Fig. 1), an identity that fixes the register of α and β strands in the C-terminal half of the P_2ase and corroborates the choice of His-392 as the second active-site histidine.

It is interesting to note that two loops implicated in the self-association of yeast PGM subunits (11) are substantially different in the projected rat Fru-2,6-P_2ase domain: (*i*) residues 69–75 in yeast PGM are involved in an extended dimer interface, and (*ii*) residues 133–140 form a weak, additional contact between dimers in the PGM tetramer. In both cases, Fru-2,6-P_2ase has severely abbreviated loops that would not favor dimer association as found in PGM.

Possible Evolutionary Link Between Mutases, P_2ases, and Acid *P*ases. Acid *P*ases catalyze phosphoryl transfers to H_2O and some alcohol acceptors; unlike alkaline *P*ases which utilize a serine residue (32), the obligatory acid *P*ase phosphoenzyme intermediate proceeds through the transient phosphorylation of a histidine residue (12). This functional similarity with the catalytic mechanism of mutases and P_2ases (9, 10) led us to explore whether there was any similarity at either the amino acid sequence or predicted secondary structure level with acid *P*ases.

Several acid *P*ase isozyme genes from yeast have been cloned and sequenced: *Saccharomyces cerevisiae pho5* and *pho3* (33, 34) and *Schizosaccharomyces pombe pho1* (35). In addition, an N-terminal fragment from the *E. coli appA* gene product (pH 2.5 acid *P*ase) is known (36). Most recently, the complete cDNA sequences of the human lysosomal and prostatic acid *P*ases have been determined (37, 38).

A gapped alignment of the available acid *P*ase sequences shows that the yeast, *E. coli*, and human enzymes are distantly related (Fig. 3). Intriguingly, the regions surrounding two conserved histidine residues, typically spaced about 240–260 amino acids apart in the acid *P*ase alignment, show a significant degree of similarity to the active site histidine residues in the mutase/P_2ase alignment (Figs. 1–3). The N-terminal His-8/258 (yeast PGM/rat Fru-2,6-P_2ase) of the mutase/P_2ase fold, embedded in a conserved Arg-**His**-Gly-(Glu or Gln) motif, is matched by an analogous N-terminal histidine residue in a similar Arg-**His**-Gly-(Glu or Asp) acid

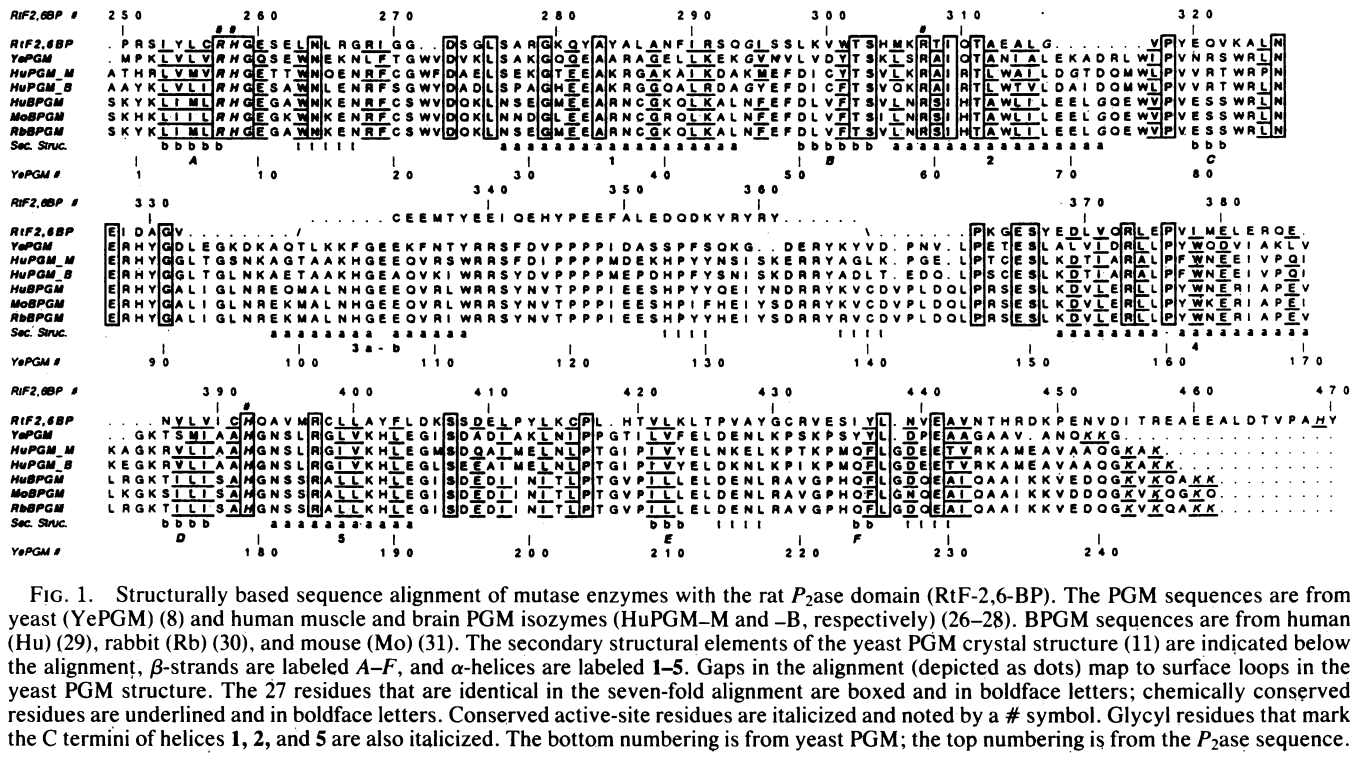

FIG. 1. Structurally based sequence alignment of mutase enzymes with the rat P_2ase domain (RtF-2,6-BP). The PGM sequences are from yeast (YePGM) (8) and human muscle and brain PGM isozymes (HuPGM–M and –B, respectively) (26–28). BPGM sequences are from human (Hu) (29), rabbit (Rb) (30), and mouse (Mo) (31). The secondary structural elements of the yeast PGM crystal structure (11) are indicated below the alignment, β-strands are labeled *A–F*, and α-helices are labeled **1–5**. Gaps in the alignment (depicted as dots) map to surface loops in the yeast PGM structure. The 27 residues that are identical in the seven-fold alignment are boxed and in boldface letters; chemically conserved residues are underlined and in boldface letters. Conserved active-site residues are italicized and noted by a # symbol. Glycyl residues that mark the C termini of helices **1**, **2**, and **5** are also italicized. The bottom numbering is from yeast PGM; the top numbering is from the P_2ase sequence.

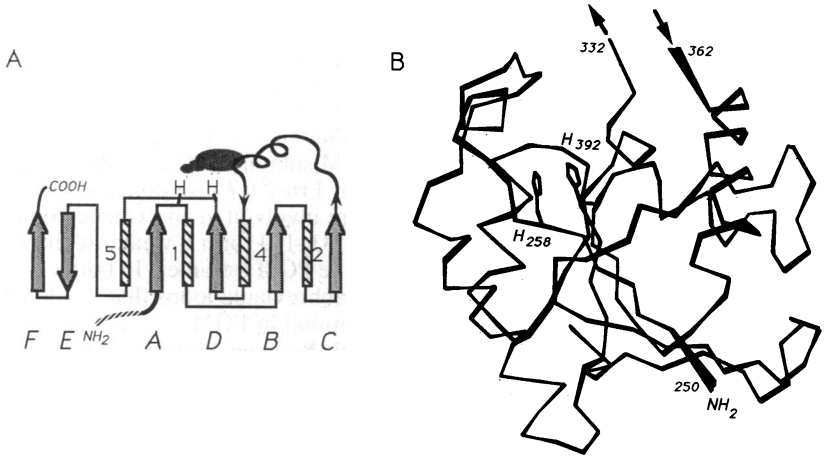

FIG. 2. (*A*) The α/β topology diagram of the shared PGM fold of mutases and P_2ases. Secondary structure is labeled as in Fig. 1; β-strands are depicted as arrows and α-helices as striped rectangles. The positions of the active-site histidine residues are noted as well as the presumed location of the Fru-2,6-P_2 molecule in the active site. The domain excursion is pictured as a loose coil distinct from the core α/β PGM fold. (*B*) Computer graphics picture of the rat Fru-2,6-P_2ase domain modeled on the backbone of yeast PGM (11). The C_α core strand "ribbon" tracing is shown for rat residues 250–443. The side chains of active-site His-258 and His-392 residues are noted. The large excursion (residues 333–361) is not modeled; the "beginning" and "end" of this coil are noted by arrows.

*P*ase motif. By analogy with PGM and Fru-2,6-P_2ase, we propose that this N-terminal acid *P*ase histidine residue is involved in the phosphoenzyme intermediate (12).

A merged alignment of mutase, Fru-2,6-P_2ase, and acid *P*ase sequences (Fig. 3) shows that predicted acid *P*ase core α and β secondary structural elements match those in yeast PGM. In addition, significant sequence similarity is observed in regions distinct from the active-site histidine residues.

The striking difference in chain length between proposed active-site histidine residues in the acid *P*ase and mutase/P_2ase sequences map to two excursions from the core α/β PGM fold: (*i*) a loop distal from the predicted active site, between helix **1** and strand *B*; and (*ii*) the variable mutase/P_2ase chain between strand *C* and helix **4** (Figs. 1–3). We conclude that the acid *P*ase family of enzymes is distantly related to the mutase/P_2ase group and suggest that they share a common protein fold with yeast PGM.

Postulated Nucleotide-Binding Fold in the Kinase Domain. A secondary structure analysis of the N-terminal half of rat 6-*P*F-2-K/Fru-2,6-P_2ase (residues 1–249) concluded that much of this region consisted of alternating α and β structure and probably folded into a conformation analogous to other nucleotide binding domains (13). The beginning of the kinase nbf could be accurately marked on the protein chain by the sequence $\overset{48}{\text{Gly}}$-Leu-Pro-Ala-Arg-$\overset{53}{\text{Gly}}$-Lys-Thr, a pattern similar to "signature" sequences diagnostic of nbfs (39, 40). This sequence motif is typically found in kinase and dehydrogenase structures marking the tight turn following the first core β-strand of the nbf (13, 39, 40).

A second characteristic sequence pattern in nbfs is associated with the "crossover" of strands that occurs when the β-sheet reverses direction, bringing to bear a strand distant in sequence to pair with the first core β-strand (13, 39, 40). This distinctive maneuver, due to the innate curl of the individual β-strands, creates a convenient cavity at the C terminus of the parallel β-sheet that most often is the active site for nbfs (13, 25). In the rat 6-*P*F-2-K sequence, the best candidate region is $\overset{121}{\text{Arg}}$-Glu-Glu-$\overset{124}{\text{Gly}}$-His-Val-Ala-Val-Phe-$\overset{130}{\text{Asp}}$, a pattern ≈75 residues C-terminal of the signature turn.

Various ATP-binding protein structures (21, 25) were then examined as models for the 6-*P*F-2-K nbf topology. Surprisingly, an N-terminal domain from the 6-*P*F-1-K bacterial structures (14, 21) provided the most convincing framework for the rat kinase domain. An alignment of spatially equivalent 6-*P*F-1-K domain residues to the noted nbf patterns in the rat 6-*P*F-2-K revealed a greater similarity in the register of observed and predicted α-helices and β-strands (Fig. 4 *Left*). Following the 6-*P*F-1-K chain past strand *D* (positioned next to strand *A* in space), a locally rich area of sequence similarity is found: rat 6-*P*F-2-K residues 148–162 (Glu-His-Gly-Tyr-Xaa$_6$-Ser-Ile-Cys-Asn-Asp) match the *Bacillus* 6-*P*F-1-K residues 114–129 (Glu-His-Gly-Phe-Xaa$_7$-Thr-Ile-Asp-Asn-Asp). The latter motif forms part of the active site cavity of 6-*P*F-1-K (21). Interestingly, this places Cys-160 of 6-*P*F-2-K in a catalytically sensitive position [consistent with

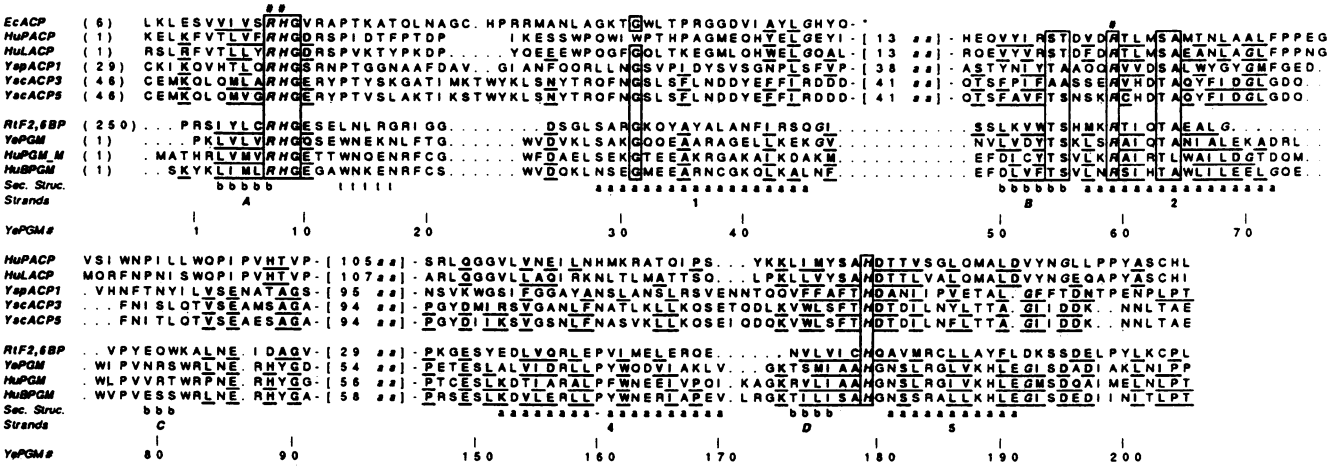

FIG. 3. Alignment of acid *P*ase sequences with the rat Fru-2,6-P_2ase domain and representative mutases. The *S. cerevisiae* (YscACP3,5) (33, 34), *S. pombe* (YspACP1) (35), human lysosomal (HuLACP) (37) and prostatic (HuPACP) (38) acid *P*ases, and the N-terminal segment of the *E. coli* acid *P*ase (EcACP) (36) are arrayed over the aligned rat Fru-2,6-P_2ase, yeast and human muscle PGMs, and the human BPGM sequences (see Fig. 1 for abbreviations). The yeast PGM numbering is followed; identities and conserved residues are marked as in Fig. 1.

the findings of El-Maghrabi *et al.* (42)]. The corresponding *E. coli* 6-*P*F-1-K Asp-127 appears to serve as a base catalyst in the kinase reaction mechanism (21).

The sequence and proposed structural similarity between 6-*P*F-2-K and the 6-*P*F-1-K family extends past strand *F* in the bacterial 6-*P*F-1-K structures to amino acid ≈201 in rat 6-*P*F-2-K (Fig. 4 *Right*). Strand *F*, however, is the first strand of a second parallel β-sheet domain that is in spatial opposition to the N-terminal, larger α/β fold in the 6-*P*F-1-K structure (14, 21). The smaller four β-strand domain of 6-*P*F-1-K extends over ≈100 residues before the protein chain rejoins the fold of the larger domain (14, 21). This chain construction is clearly incompatible with the remaining ≈45 residues available to the 6-*P*F-2-K domain before linking with the P_2ase fold. The crystal structure of *E. coli* 6-*P*F-1-K complexed with Fru-1,6-P_2, ADP, and Mg^{2+} (21) shows that the larger domain contributes most of the residues that bind the nucleotide moiety, while the sugar-phosphate molecule is contacted by residues from both the large and small domains of 6-*P*F-1-K (25). The rat kinase domain may form a (more economical and unrelated) structural and functional counterpart to the 6-*P*F-1-K small domain excursion (Fig. 4 *Right*).

The N-terminal ≈40 amino acids of rat 6-*P*F-2-K do not form an integral part of the model nbf domain. Conformational changes following phosphorylation of Ser-32 by the cAMP-dependent protein kinase (6) may propagate through the sequence-proximal strand *A* (Fig. 4), disrupting the predicted, spatially distant ATP/Fru-6-*P* binding cavity at the C terminus of the core β-sheet.

DISCUSSION

Predictive structural studies of the bifunctional enzyme 6-*P*F-2-K/Fru-2,6-P_2ase reveal differing traces of evolutionary lineage with two glycolytic enzymes and a family of monophosphoesterases that catalyze a phosphoryl transfer reaction. In this report we argue that the C-terminal P_2ase domain of 6-*P*F-2-K/Fru-2,6-P_2ase is homologous to the mutase family of enzymes. The P_2ase structure can be convincingly modeled on the template backbone of the yeast PGM fold (Fig. 2). This allows the three-dimensional, comparative mapping of residues that populate the active site crevices of yeast PGM and the rat Fru-2,6-P_2ase domain.

Models of the catalytic mechanism of mutases do not generally involve residues other than the two closely spaced histidine imidazole rings with any degree of certainty (11). Otherwise, spatial proximity to the active site histidine residues has been inferred as the only arbiter of catalytic importance (11): conserved mutase residues Arg-7, Arg-59, and Glu-86 are shared by the P_2ase (Fig. 1). These identities aside, we expect that subtle amino acid differences in the active site periphery may be responsible for shifting the catalytic efficiency of a generic PGM-fold enzyme towards one of three reactions: mutase, *P*ase, or synthase (44). Yeast and human PGMs represent examples of enzymes that favor the mutase activity (26–28, 44); BPGM is preferentially a synthase (28, 44), while the P_2ase domain of rat 6-*P*F-2-K/Fru-2,6-P_2ase primarily carries out the *P*ase reaction for both fructose and glycerate substrates (45). Each of the three classes of PGM-fold enzymes can, with diminished capacity, carry out the other two reactions (44). Some indication of this specialization comes from the isolation of an Arg-89 → Cys variant of human BPGM (46) (see Fig. 1). Both mutase and synthase activities are decreased to 5% and 10% of wild type, respectively, while the *P*ase activity is unchanged. The equivalent residue in the bifunctional enzyme is Ile-328 (Fig. 1), suggesting that a reverse mutation of Ile-328 → Arg may enhance the mutase and synthase reactions in the Fru-2,6-P_2ase.

We propose that both the P_2ase and mutase families are in turn distantly related to a family of acid *P*ases. All of these enzymes have in common a phosphohistidine intermediate in their phosphotransfer reactions (9, 10, 12). Based on the structural similarities that we have postulated between acid *P*ases and the PGM fold, it is likely that the acid *P*ase phosphoacceptor histidine is located in the conserved N-terminal Arg-**His**-Gly motif (Fig. 3).

There is great diversity in the excursions from the core fold in each of the three PGM-like enzyme classes. The prominent structural difference between mutases and the rat Fru-2,6-P_2ase domain maps to the chain segment between core β-strand *C* and helix **4** that forms a lobe overhanging the

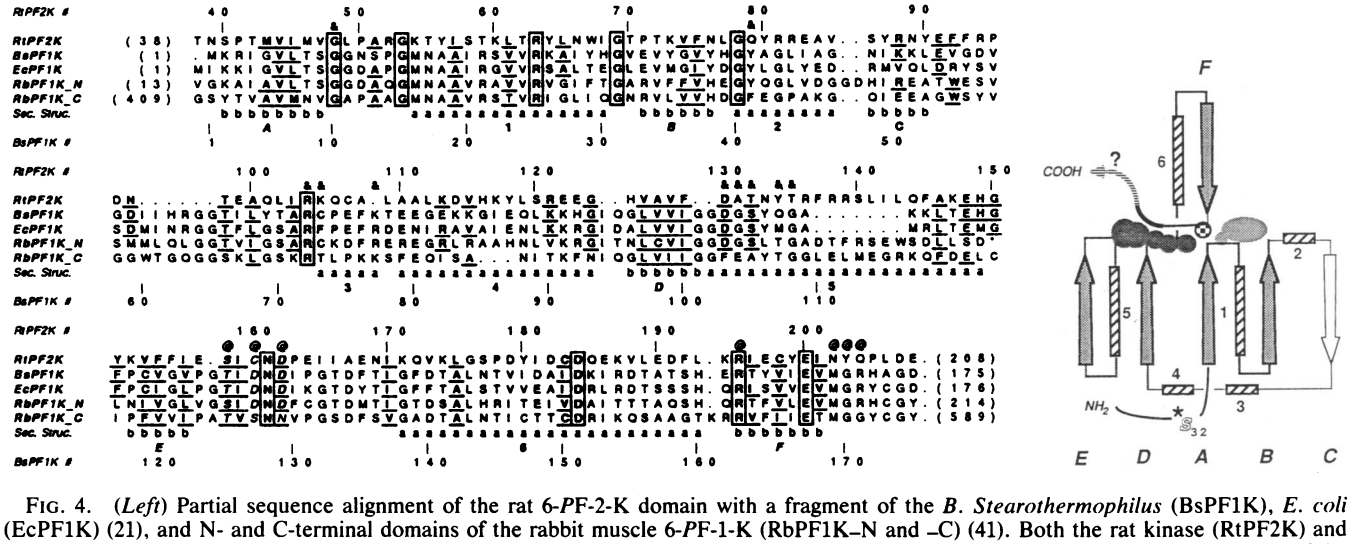

FIG. 4. (*Left*) Partial sequence alignment of the rat 6-*P*F-2-K domain with a fragment of the *B. Stearothermophilus* (BsPF1K), *E. coli* (EcPF1K) (21), and N- and C-terminal domains of the rabbit muscle 6-*P*F-1-K (RbPF1K–N and –C) (41). Both the rat kinase (RtPF2K) and BsPF1K numbering schemes are used. Note that the 6-*P*F-2-K sequence similarity is poor in the region of the edge β-strand (labeled *C*) of the β-sheet of the 6-*P*F-1-K large domain (21); as a result, the topology of this edge strand is uncertain in the kinase model (see *Right*). Identities and conserved residues are as in Fig. 1. The symbols & and @ denote 6-*P*F-1-K residues that are involved in ADP or Fru-1,6-P_2 binding, respectively (21). The (italicized) catalytic 6-*P*F-1-K residue Asp-127 is matched by Cys-160 in the rat kinase domain. The * symbol in the RbPF1K–N sequence marks the loop insertion of 17 residues at position 150 (41). (*Right*) A proposed (partial) topology for the rat 6-*P*F-2-K domain based on similarity with the 6-*P*F-1-K crystal structure (21). The regions of best similarity are in bold; the edge strand *C* and surrounding chain is in lighter relief. The β-strands and α-helices are labeled as in ref. 21. The approximate positions of the ATP (dark shading), Mg^{2+} ion (checkered circle) and Fru-6-*P* (light shading) are indicated in the putative active-site region by analogy with 6-*P*F-1-K (21).

active site in yeast PGM (11) (Figs. 1 and 2). This extruded structure is dispensable for the formation of a hydrophobic core in the α/β fold of yeast PGM and the model Fru-2,6-P_2ase domain (Fig. 2). It is of interest to test whether these appended lobes of dissimilar structure are unnecessary to enzyme function or instead serve to divergently modulate catalytic activity or quaternary interactions. This situation is reminiscent of the length variable, nonhomologous excursions from the nbf core that are seen in aminoacyl tRNA synthetases (47).

The kinase domain of 6-*P*F-2-K/Fru-2,6-P_2ase is proposed to display partial structural similarity to the functionally analogous domain of 6-*P*F-1-K (Fig. 4). This similarity may be indicative of convergence at the active site of two enzymes that bind a similar array of ligands and catalyze a similar kinase reaction (25). One proposal of the 6-*P*F-2-K modeling study concerns the need for dimerization of kinase domains for kinase activity, as many residues that contribute to the active site of the neighboring kinase in the 6-*P*F-1-K complex are predicted to be conserved, as well as the secondary structural elements that form the dimer interface (16). These findings are consistent with experiments that have tested the kinase and P_2ase activity of separately expressed rat liver 6-*P*F-2-K and Fru-2,6-P_2ase domains (48, 49). While both domains are independently catalytically competent, the 6-*P*F-2-K domain forms a dimer (or greater aggregate), while the P_2ase remains monomeric in solution (49).

Experiments of Tauler *et al.* (45, 48, 49) illustrate steps in the likely evolutionary path that we have drawn for the bifunctional 6-*P*F-2-K/Fru-2,6-P_2ase enzyme. The observed catalytic independence of fused domains is consistent with the proposed, distinct structural designs of a 6-*P*F-1-K-analogous kinase and a PGM-homologous P_2ase. Further clues to the evolutionary history of this bifunctional enzyme may be provided by the partial gene structure of the rat liver 6-*P*F-2-K/Fru-2,6-P_2ase (43). While no intron marks the sequence division of kinase/P_2ase domains, two other gene segments are of particular interest: the N-terminal 32 amino acids [including the phosphorylated Ser-32 residue (6)] that precede the proposed kinase domain are separately exon-encoded, as is the large excursion from the core PGM fold in the P_2ase domain. These regions of the bifunctional enzyme may represent structurally dispensable but functionally important later additions to the separate domains.

We thank Drs. A. Tauler, A. Lange, I. Kurland, R. El-Maghrabi, P. Evans, M. Browner, and T. Claus for constructive criticism during the preparation of this manuscript. J.F.B. acknowledges the financial support of Tina S. Bazan and a National Institutes of Health Predoctoral Training Grant.

1. Pilkis, S. J., Claus, T. H., Kountz, P. D. & El-Maghrabi, M. R. (1987) in *The Enzymes*, ed. Boyer, P. (Academic, New York), 3rd Ed., Vol. 28, pp. 3–45.
2. Pilkis, S. J., Fox, E., Wolfe, L., Rothbart, L., Colosia, A., Stewart, H. B. & El-Maghrabi, M. R. (1986) *Ann. NY Acad. Sci.* **478,** 1–19.
3. Pilkis, S. J., Regen, D. M., Stewart, H. B., Pilkis, J., Pate, T. M. & El-Maghrabi, M. R. (1984) *J. Biol. Chem.* **259,** 949–958.
4. El-Maghrabi, M. R., Pate, T. M., Murray, K. J. & Pilkis, S. J. (1984) *J. Biol. Chem.* **259,** 13096–13103.
5. Pilkis, S. J., Regen, D. M., Stewart, H. B., Chrisman, T., Pilkis, J., Kountz, P., McGrane, M., El-Maghrabi, M. R. & Claus, T. H. (1983) *Mol. Asp. Cell. Regul.* **3,** 95–102.
6. Murray, K. J., El-Maghrabi, M. R., Kountz, P. D., Lukas, T. J., Soderling, T. R. & Pilkis, S. J. (1984) *J. Biol. Chem.* **259,** 7673–7681.
7. Lively, M. O., El-Maghrabi, M. R., Pilkis, J., D'Angelo, G., Colosia, A. D., Ciavola, J.-A., Fraser, B. A. & Pilkis, S. J. (1988) *J. Biol. Chem.* **263,** 839–849.
8. Fothergill, L. A. & Harkins, R. N. (1982) *Proc. R. Soc. London B* **215,** 19–44.
9. Rose, Z. B. (1980) *Adv. Enzymol.* **51,** 211–253.
10. Pilkis, S. J., Lively, M. O. & El-Maghrabi, M. R. (1987) *J. Biol. Chem.* **262,** 12672–12675.
11. Winn, S. I., Watson, H. C., Harkins, R. N. & Fothergill, L. A. (1981) *Philos. Trans. R. Soc. London B* **293,** 121–130.
12. Van Etten, R. L. (1982) *Ann. NY Acad. Sci.* **390,** 27–51.
13. Rossman, M. G., Liljas, A., Branden, C.-I. & Banaszak, L. J. (1975) in *The Enzymes*, ed. Boyer, P. (Academic, New York), 3rd Ed., Vol. 11, pp. 61–102.
14. Evans, P. R. & Hudson, P. J. (1979) *Nature (London)* **279,** 500–504.
15. Bazan, J. F. & Fletterick, R. J. (1988) *Proc. Natl. Acad. Sci. USA* **85,** 7872–7876.
16. Bazan, J. F. & Fletterick, R. J. (1989) in *Fructose-2,6-Bisphosphate*, ed. Pilkis, S. J. (CRC, Boca Raton, FL), in press.
17. Devereaux, J., Haeberli, P. & Smithies, O. (1984) *Nucleic Acids Res.* **10,** 703–795.
18. Gribskov, M., McLachlan, A. D. & Eisenberg, D. (1987) *Proc. Natl. Acad. Sci. USA* **84,** 4355–4358.
19. Taylor, W. R. (1988) *Prot. Eng.* **2,** 77–86.
20. Jones, T. A. (1982) in *Computational Crystallography*, ed. Sayre, D. (Oxford Univ. Press, Oxford), pp. 303–317.
21. Shirakihara, Y. & Evans, P. R. (1988) *J. Mol. Biol.* **204,** 973–994.
22. Bernstein, F. C., Koetzle, T. F., Williams, G. J. B., Meyer, E. F., Jr., Brice, M. D., Rogers, J. R., Kennard, O., Shimanouchi, T. & Tasumi, M. (1977) *J. Mol. Biol.* **112,** 535.
23. Ponder, J. W. & Richards, F. M. (1987) *J. Mol. Biol.* **193,** 775–791.
24. Summers, N. L., Carlson, W. D. & Karplus, M. (1987) *J. Mol. Biol.* **196,** 175–198.
25. Branden, C.-I. (1980) *Q. Rev. Biophys.* **13,** 317–338.
26. Shanske, S., Sakoda, S., Hermodson, M. A., DiMauro, S. & Schon, E. A. (1987) *J. Biol. Chem.* **262,** 14612–14617.
27. Sakoda, S., Shanske, S., DiMauro, S. & Shon, E. A. (1988) *J. Biol. Chem.* **263,** 16899–16905.
28. Bloquit, Y., Calvin, M.-C., Rosa, R., Prome, D., Prome, J.-C., Prathernou, F., Cohen-Solal, M. & Rosa, J. (1988) *J. Biol. Chem.* **263,** 16906–16910.
29. Joulin, V., Peduzzi, J., Romeo, P.-H., Rosa, R., Valentin, C., Dubart, A., Lapeyre, B., Bloquit, Y., Garel, M.-C., Goosens, M., Rosa, J. & Cohen-Solal, M. (1986) *EMBO J.* **5,** 2275–2283.
30. Yanagawa, S. I., Hitomi, K., Sasaki, R. & Chiba, H. (1986) *Gene* **44,** 185–191.
31. Le Boulch, P., Joulin, V., Garel, M.-C., Rosa, J. & Cohen-Solal, M. (1988) *Biochem. Biophys. Res. Commun.* **156,** 874–881.
32. Sowadski, J. M., Handschumacher, M. D., Krishna Murthy, H. M., Foster, B. A. & Wyckoff, H. W. (1985) *J. Mol. Biol.* **186,** 417–433.
33. Bajwa, W., Meyhack, B., Rudolph, H., Schweingruber, A.-M. & Hinnen, A. (1984) *Nucleic Acids Res.* **12,** 7721–7739.
34. Arima, K., Oshima, T., Kubota, I., Nakamura, N., Mizunaga, T. & Tohe, A. (1983) *Nucleic Acids Res.* **11,** 1657–1672.
35. Elliot, S., Chang, C.-W., Schweingruber, M. E., Schaller, J., Rickli, E. E. & Carbon, J. (1986) *J. Biol. Chem.* **261,** 2936–2941.
36. Touati, E. & Danchin, A. (1987) *Biochimie* **69,** 215–221.
37. Pohlmann, R., Krentler, C., Schmidt, B., Schroder, W., Lorkowski, G., Culley, J., Mersmann, G., Geier, C., Waheed, A., Gottschalk, S., Grzeschik, K.-H., Hasilik, A. & von Figura, K. (1988) *EMBO J.* **7,** 2343–2350.
38. Vihko, P., Virkunnen, P., Henttu, P., Roiko, K., Solin, T. & Huhtala, M.-L. (1988) *FEBS Lett.* **236,** 275–281.
39. Moller, W. & Amons, R. (1985) *FEBS Lett.* **186,** 1–7.
40. Wierenga, R. K., Terpstra, P. & Hol, W. G. H. (1986) *J. Mol. Biol.* **187,** 101–107.
41. Lee, C.-P., Kao, M.-C., French, B. A., Putney, S. D. & Chang, S. H. (1987) *J. Biol. Chem.* **262,** 4195–4199.
42. El-Maghrabi, M. R., Pate, T. M., D'Angelo, G., Correia, J. J., Lively, M. O. & Pilkis, S. J. (1987) *J. Biol. Chem.* **262,** 11714–11720.
43. Lange, A. J., Kummel, L., El-Maghrabi, M. R., Tauler, A., Colosia, A., Marker, A. & Pilkis, S. J. (1989) *Biochem. Biophys. Res. Commun.* **162,** 753–760.
44. Rose, Z. B. (1982) *Methods Enzymol.* **87,** 42–51.
45. Tauler, A., El-Maghrabi, M. R. & Pilkis, S. J. (1987) *J. Biol. Chem.* **262,** 16808–16815.
46. Rosa, R., Bloquit, Y., Calvin, M.-C., Prome, D., Prome, J.-C. & Rosa, J. (1989) *J. Biol. Chem.* **264,** 7837–7843.
47. Starzyk, R. M., Webster, T. A. & Schimmel, P. (1987) *Science* **237,** 1614–1618.
48. Tauler, A., Rosenberg, A. H., Colosia, A., Studier, F. W. & Pilkis, S. J. (1988) *Proc. Natl. Acad. Sci. USA* **85,** 6642–6646.
49. Tauler, A., Lange, A. J., El-Maghrabi, M. R. & Pilkis, S. J. (1989) *Proc. Natl. Acad. Sci. USA* **86,** 7316–7320.